ELSEVIER

Contents lists available at ScienceDirect

Construction and Building Materials

journal homepage: www.elsevier.com/locate/conbuildmat





Effect of internal curing on shrinkage and cracking potential under autogenous and drying conditions

Bayram Tutkun^{a,*}, Ege Su Barlay^b, Çağlar Yalçınkaya^b, Halit Yazıcı^b

- ^a Institute of Material Technology, Building Physics, and Building Ecology, Faculty of Civil Engineering, TU Wien, Vienna. Austria
- ^b Department of Civil Engineering, Faculty of Engineering, Dokuz Eylül University, İzmir, Türkiye

ARTICLE INFO

Keywords:
Autogenous shrinkage
Drying shrinkage
Internal curing
Superabsorbent polymers (SAP)
Cracking
Steel fiber reinforced cementitious composites

ABSTRACT

Autogenous shrinkage is a significant issue in ultra-high-performance concrete (UHPC). Internal curing has been effective in mitigating autogenous shrinkage, but its impact on drying shrinkage and crack-free concrete needs to be considered. This study investigates the controversial phenomenon of the effect of internal curing on shrinkage strains under drying conditions. A very specific steel fiber reinforced cementitious composite (Slurry infiltrated fiber concrete (SIFCON)) was examined to better understand the cumulative effects. Two additional internal curing water contents (36 kg/m³ and 60 kg/m³) and two superabsorbent polymers (SAP) with different particle sizes (D_{50} : 215 μm and D_{50} : 725 μm) were utilized. Shrinkage measurements were conducted on the SIFCON matrix for early (up to 7 days) and long-term (up to 90 days), under both autogenous and drying conditions. The SIFCON specimens were cured under autogenous and drying conditions for 90 days, then dried to simulate the field conditions, which was followed by crack mapping. The results indicate that SAP effectively mitigates shrinkage strains under both autogenous and drying conditions, attributed to its ability to reduce plastic shrinkage strains during the initial hours. However, crack mapping studies revealed increased cracked areas in specimens with SAP usage, higher internal curing water content, and larger SAP size. Additionally, specimens cured under autogenous conditions exhibited more cracks compared to those cured under drying conditions. This suggests that although shrinkage measurements demonstrate positive effects of internal curing in both conditions, the cumulative effect can vary.

1. Introduction

Material technology has been rapidly developing over the past few decades due to continuous demand. Concrete, among other materials, still holds its position as the most successful and widely used human-made material [1]. With the high consumption and demand, researchers have been developing various types of ultra-high-performance concrete (UHPC). In addition to their impressive mechanical properties, these new materials are also expected to be long-lasting, considering the limitations of our world's resources. The term "high-performance" in UHPC refers to its remarkable durability properties besides advanced mechanical properties. In addition to conventional construction purposes, UHPC offers tailor-made solutions such as high-early strength [2], high ductility [3], and impact resistance [4].

However, dimensional stability is the Achilles tendon of UHPC. Although UHPC is designed to resist external forces, internal forces such as shrinkage are more difficult to control. Most UHPC designs aim to lower the water-to-binder ratio and increase the binder dosage, but this increases the risk of shrinkage. Early-age shrinkage of concrete refers to the reduction in the volume of the concrete that occurs in freshly placed and hardening concrete during the initial stages of the curing process. Among the different types of shrinkage, plastic shrinkage, autogenous shrinkage, and drying shrinkage pose the most significant challenges for UHPC. Plastic shrinkage begins when the concrete is in its plastic state and continues for a couple of hours until the final setting. If the rate of evaporation exceeds the rate of bleeding, increased capillary pressures and volumetric consolidation lead to plastic shrinkage [5]. Autogenous shrinkage is mainly effective during the early stages of hydration, typically the first few days [6]. This time the hydration reactions are responsible for the apparent volume reduction by mainly triggering the chemical shrinkage and internal consumption of water [7]. Drying shrinkage, on the other hand, can occur throughout the lifespan of the concrete. The mechanism of drying shrinkage is based on water loss due to evaporation. The internal and external humidity of the concrete will

E-mail address: bayram.tutkun@tuwien.ac.at (B. Tutkun).

^{*} Corresponding author.

eventually reach equilibrium. Meanwhile, as water moves inside the concrete, drying shrinkage occurs during the stage of water movement through the exterior of the concrete. After the water movement, the porous skeleton shrinks due to various mechanisms such as disjoining pressure, capillary pressure, and changes in surface free energy [7].

Prevention methods for shrinkage can be categorized into active and passive methods [8]. Passive methods commonly involve optimizing mixture design or substituting materials with lower shrinkage potential for those with higher shrinkage potential (e.g., substituting fly ash for cement). Active methods focus on controlling environmental conditions. These methods are applicable to all types of shrinkage and are often the initial approaches due to their lower cost and less labor sensitivity. Admixtures can also be used as shrinkage mitigating agents, depending on the type of shrinkage. Various admixtures, such as superabsorbent polymers (SAP) [9,10], lightweight aggregates [11] or viscosity modifiers [12], and shrinkage-reducing admixtures (SRA) [13], have been found effective in mitigating plastic shrinkage regardless of their primary purpose. Similarly, internal curing agents like SAP and lightweight aggregates [14], or expansive agents [15], can be utilized to mitigate autogenous shrinkage. SRA and expansive agents are also effective in mitigating drying shrinkage [16].

Active methods primarily focus on physically preventing water loss and vary depending on the type of shrinkage to be prevented. Based on the basic mechanisms mentioned above, it can be concluded that water evaporation should be prevented to mitigate plastic and drying shrinkage. Autogenous shrinkage, however, requires special attention. As it is caused by water consumption during hydration reactions, active methods such as traditional curing methods (e.g., water-ponding, wet/moist covering, and fog spraying) can be employed to prevent it. It is worth noting that autogenous shrinkage typically does not exceed 100 $\mu\epsilon$ in normal concrete but becomes problematic in concrete with low water-to-binder ratios and high cement dosages [17].

Shrinkage is a complex phenomenon, and specific precautions need to be taken for each concrete mix and specific conditions. For instance, the impermeability of UHPC restricts the successful application of external water supply [18]. In such cases, a passive method known as internal curing can be employed to mitigate autogenous shrinkage in impermeable concrete mixes with high autogenous shrinkage potential. In 1991, Philleo [19] introduced a novel curing technique termed "internal curing." This method involves the integration of water reservoirs within the concrete to supply additional water for ongoing hydration and to counteract water loss from reactions. Materials that can absorb water and release it in a controlled manner, such as lightweight aggregates, SAP, wood fibers, powders, microcapsules, and emulsified water, are suitable as internal curing agents [20]. In his research, Philleo [19] employed lightweight aggregates for this purpose. Subsequently, pioneering studies by Tsuji et al. in 1998 [21] and Jensen and Hansen in 2002 [22] presented SAP as an effective internal curing agent. SAP has gained attention as an internal curing agent due to its significant water absorption capacity (up to 30-40 times its weight in cement pore solution [23]) and easier application compared to lightweight aggregates.

In the context of shrinkage, certain prevention methods can have both positive and negative effects on different types of shrinkage. For example, while wet covering has been observed to negatively affect drying shrinkage, it is essential to note that in an open system exposed to external relative humidity, the capillary pressure is governed by the RH. The finer pore structure on the outer surface can lead to a higher degree of saturation and smaller pore sizes, which suggests greater capillary tension-induced strain during drying [24] Similarly, the effect of internal curing on autogenous shrinkage is generally positive, but there are contradictory results regarding its effect on drying shrinkage. Some studies have reported reductions in shrinkage strains under drying conditions when internal curing methods are applied [25,26]. while others have observed increases in shrinkage strains [27,28].

The reductions in shrinkage strains under drying conditions can be linked to factors such as the increase of effective stress [29], a decrease

in the depth of drying, and minimized humidity disparities within the specimen [30]. Conversely, the escalation in shrinkage strains has been associated with a range of factors [31]. SAP serves as internal reservoirs in concrete, absorbing water during the mixing phase and subsequently dispersing it to the adjacent cement paste. However, as underscored by insights from Wyrzykowski et al. [32], even though the SAP-contained water exhibits enhanced mobility, it is the movement through the adjacent cement paste that predominantly dictates the pace. The process of self-desiccation plays a role in depleting the SAP. Moreover, the earlyage water dynamics in the cement paste might be instrumental in optimizing internal curing. Additionally, the distribution patterns of SAP within cement paste matrices indicate challenges in achieving complete coverage of the matrix, even when there is an abundance of entrained water [32]. Collectively, these observations spotlight the pivotal role of water dynamics in relation to drying shrinkage. The behavior and distribution of water might not consistently correlate with drying shrinkage patterns, underscoring the need for a deeper exploration of these mechanisms and their implications.

In the scope of this study, mechanisms, and effects of internal curing on the early and long term on both autogenous and drying shrinkage were investigated. Rather than restraining the specimens, a very specific concrete (slurry infiltrated fiber concrete (SIFCON)) might help to understand this phenomenon. SIFCON is a special type of concrete that consists of up to 30 % (by volume) fiber content [33]. To produce SIF-CON fibers are laid randomly or oriented in the mold, then a very fluid slurry is poured over these fibers. SIFCON is known for extraordinary mechanical properties; even though it deformed 10 % under flexural load, it can still maintain 60 % of its compressive strength, and in the same compressive strength class, the toughness of SIFCON can be 50 times greater than normal concrete [34]. Rather than conventional construction purposes, the aim of the SIFCON mostly covers strengthening, repairing, and impact resistance [35]. Besides these superior properties of SIFCON, it can, rarely, suffer from some durability problems such as freeze-thaw [36], sulfate attack [37], corrosion [38], and shrinkage [39]. In addition, shrinkage cracks are known to connect capillary pores to each other [40], thus, durability problems could occur. SIFCON consists of steel fibers up to 30 %, thus, impermeability is quite important since steel fibers are more sensitive to environmental attacks than normal concretes. The shrinkage properties of SIFCON are not comprehensively examined in the literature. Even though no significant shrinkage strains were observed in the SIFCON specimens, it is reported that areas between fibers are cracked [39]. It is pointing out that SIFCON potentially tends to shrinkage and shrinkage cracks. This is mostly related to the rigid and connected fiber structure of SIFCON. This unique property makes SIFCON a suitable material for studying shrinkage, especially when examining the cumulative effects of applied prevention methods.

The cumulative effects of prevention methods have not been extensively investigated in the literature. Some methods used to mitigate plastic and autogenous shrinkage may have negative effects on drying shrinkage. Internal curing, particularly the use of SAP, has been extensively studied, but its effect on shrinkage strains under drying conditions remains a research gap. This study aims to fill this gap by conducting shrinkage measurements and crack analyses on specimens subjected to autogenous and drying conditions.

2. Experimental program

2.1. Materials

CEM I 42.5 R type Portland cement with a specific surface area of $395~\text{m}^2/\text{kg}$ was supplied by Soma Cement. Silica fume (MasterRoc® MS 610) with a nitrogen absorption fineness of 20,000 m^2/kg and a SiO2 content of 92.25 % was supplied by BASF. The material properties of the cement and silica fume are presented in Table 1.

Two SAPs based on acrylamide and acrylic acid were supplied by

 Table 1

 Chemical compositions of cement and silica fume (%).

	SiO_2	Al_2O_3	Fe_2O_3	CaO	MgO	Na ₂ O	K_2O	SO_3	Cl ⁻	LOI
Cement	19.79	4.78	3.39	63.71	1.78	0.32	0.78	2.84	0.0098	2.09
Silica Fume	92.25	0.88	1.98	0.51	0.96	0.45	0.12	0.33	-	_

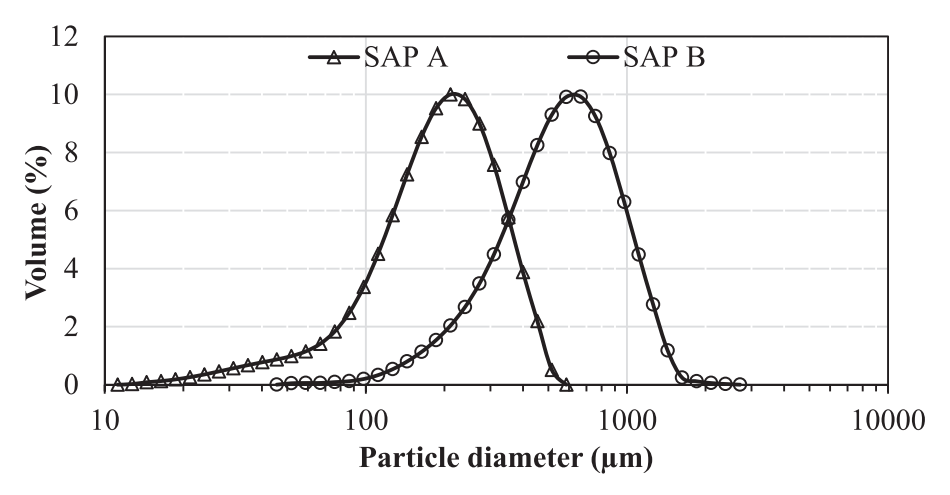


Fig. 1. Particle size distributions of SAP A and SAP B.

SNF Floerger (France). The SAP with a smaller particle size, having a D_{50} value of 215 μm , was named SAP A, while the SAP with a larger particle size, having a D_{50} value of 725 μm , was named SAP B. The particle size distributions of the SAPs were determined using a Master Sizer Hydro 3000 model particle size analyzer. The water absorption kinetics of these SAPs have been previously investigated in a previous study [41]. The particle size distributions of the SAPs are presented in Fig. 1.

The experimental studies involved the use of three different sizes of quartz aggregate (0.4–1, 0–0.4, and 0–0.075 mm). The specific gravity of the quartz aggregate was 2.61, with a water absorption of 0.10 %. To ensure proper filling of the SIFCON slurry into the dense fibers, a finer aggregate gradation was preferred, and the maximum aggregate size was limited to 1 mm. To achieve the desired fresh-state properties without experiencing bleeding and segregation, a polycarboxylic etherbased high-range water reducer (MasterGlenium® ACE 450) supplied by BASF was added to the SIFCON matrix. For the compressive strength and crack mapping studies, hooked-end steel fibers 35 mm in length and 0.55 mm in diameter were employed. The steel fibers had an aspect ratio of 45 and a tensile strength of 1200 MPa.

2.2. Mixture designs and mixing procedure

A SIFCON matrix was designed with specific ratios: a water/cement ratio of 0.28, a water-to-binder ratio of 0.25, and a water-to-powder

ratio of 0.18. The volume of fibers in the mixture was set at 10 % (by volume), and fibers were randomly distributed. Only the fiber orientation is determined before the trials. Fiber volume is ascertained by placing fibers, dispersed randomly, into the respective molds intended for the experiments. Subsequently, the total fiber ratio filling the molds entirely is calculated. The mix designs for the SIFCON are presented in Table 2. In the mixture codes, the first part denotes the type of SAP (A or B), while the second part indicates the amount of internal curing water (36 or 60 kg/m³). The volumes of aggregate and cement were kept constant for the SAP-modified mixtures. Additional curing water was added on top of the mixing water. Thus, for a 1 m³ mixture, the mix designs were slightly changed. However, these changes were minor, and it was assumed that the internal curing water would remain contained within the SAP until required. Similar methodologies have been applied in previous studies [42,43].

Based on Jensen and Hansen's approach [44] (Eq. (1), the theoretical requirement for additional internal curing water was calculated to be 36 kg/m 3 . However, considering that the actual conditions did not perfectly match the ideal conditions of complete cement hydration and uniform water access to all cement particles, a higher amount of additional internal curing water (60 kg/m 3) was also selected. As a result, two different amounts of additional internal curing water (36 kg/m 3 and 60 kg/m 3) were employed for both types of SAP.

Table 2Mixture designs and properties.

	REF	SAP A 36	SAP B 36	SAP A 60	SAP B 60
Cement (kg/m³)	800	800	800	800	800
Silica Fume (kg/m ³)	80	80	80	80	80
Additional Internal Curing Water (kg/m ³)	_	36	36	60	60
Total Water (kg/m ³)	220	256	256	280	280
SAP (kg/m^3)	_	0.90	1.09	1.50	1.82
Quartz (0–0.075 mm) (kg/m^3)	328	328	328	328	328
Quartz (0-0.4 mm) (kg/m ³)	419	419	419	419	419
Quartz (0.4–1 mm) (kg/m ³)	140	140	140	140	140
Steel Fiber (kg/m ³)	785	785	785	785	785
Superplasticizer (kg/m ³)	17	17	17	17	17
Free Flow Diameter (cm)	34.5 (±0.71)	30.8 (±0.57)	32.8 (±0.42)	31.3 (±0.42)	31.0 (±0.49)
Mini V-funnel Passing Time (s)	13.8 (±0.35)	19.3 (±0.39)	12.3 (± 0.45)	13.7 (± 0.35)	12.9 (±0.30)
Compressive Strength (MPa)	142.9 (±4.5)	125.2 (±3.6)	123.0 (± 6.8)	113.9 (±3.1)	114.8 (±5.2)

$$(w/c)_e = \begin{cases} 0.18(w/c); forw/c < 0.36 \\ 0.42 - (w/c); for 0.36 \le w/c \le 0.42 \\ 0; forw/c > 0.42 \end{cases} \tag{1}$$

where: $(w/c)_e = additional$ water needed for internal curing (g of water per g of cement)

The absorbency values for SAP A and SAP B were assessed using the slump flow method, which is commonly employed for mixtures containing SAP [23]. To match the slump values with the reference mixtures, water was added to the SAP-containing mixtures, and the slump flow test was conducted on standard mortar mixtures with a water-to-cement ratio of 0.5 and quartz aggregate with standard gradation. Following 15 drops, the flow values were determined in accordance with the TS EN 1015–3 standard [45]. Based on the results of the slump flow test, the absorbency values for SAP A and SAP B were found to be 40 g/g and 33 g/g, respectively. Regarding the SAP A 36 and SAP A 60 mixtures, the quantities of SAP utilized were 0.11 % and 0.19 % (by weight of cement), respectively. Similarly, for the SAP B 36 and SAP B 60 mixtures, the amounts of SAP employed were 0.14 % and 0.23 % (by weight of cement), respectively. These proportions were determined based on the absorbency rates obtained through the slump flow method.

A Hobart mixer with a 2-liter capacity was employed to prepare the mixtures. For the internal curing mixtures, SAP was added to the mixtures in dry form, and the additional internal curing water was weighed together with the mixture water. The dry ingredients of the mixture were pre-mixed for 1 min. Then, 2/3 of the water and the superplasticizer were added to the mixture, with the remaining 1/3 of the water added separately. The mixture, along with the water and superplasticizer, was mixed at normal speed for 9 min, followed by an additional 9 min of high-speed mixing.

Given the SIFCON matrix's high powder content and a relatively substantial amount of superplasticizer, prolonged mixing periods were preferred to ensure homogeneous dispersion of the superplasticizer. Once the mixing process was completed, the SIFCON slurry was poured into molds that had been pre-filled with 10 % (by volume) steel fibers for compressive strength and crack mapping studies. On the other hand, for the early and long-term specimens, fibers were not utilized, as the study aimed to examine the slurry's shrinkage strains. To ensure proper filling of the slurry between the fibers, it was gradually placed in 10 steps, without employing any vibration.

The workability of the mixtures was evaluated through the free flow test and mini v-funnel test, following the EFNARC guidelines [46]. Compressive strength values were determined on $71 \times 71 \times 71$ mm cube specimens after 28 days of standard water curing. To eliminate the possibility of misleading results arising from internal humidity variations due to the presence of SAP, as emphasized by Esteves et al. [47], the specimens were further subjected to drying in a 40 °C oven for three days. A temperature of 40 °C can be a detrimental drying condition,

potentially leading to the emergence of fine cracks. For mixtures like SIFCON, drying specimens presents challenges due to their impermeable characteristics. After a series of initial trials, the minimum drying degree was determined. Nonetheless, drying attempts in a 40 $^{\circ}\text{C}$ environment did not successfully dry the specimens completely. The workability and compressive strength results are presented in Table 2.

2.3. Early age shrinkage measurements

Early age shrinkage measurements were carried out using a non-contact laser system for a period of up to 7 days from the initial setting time. This system has been successfully implemented in previous publications [48,49]. Each mixture was assessed using five specimens with dimensions of $25 \times 25 \times 290$ mm for the early age shrinkage measurements. Since notable length changes were not expected in SIF-CON mixtures and the objective was to observe the effect of the matrix's shrinkage between fibers, only the SIFCON matrix (without fibers) was examined in this section of the study.

For the autogenous shrinkage measurements, the shrinkage system was maintained at a temperature of 20 $^{\circ}\text{C}$ and a relative humidity of 95 %. Furthermore, to prevent any water evaporation, the molds were covered with parafilm, in addition to the ambient system conditions. Regarding the drying shrinkage measurements, the shrinkage system was set at a temperature of 20 $^{\circ}\text{C}$ and a relative humidity of 50 %. An illustration of the non-contact laser system is presented in Fig. 2.

2.4. Long-term shrinkage measurements

Long-term shrinkage measurements were conducted on three mortar bar specimens with dimensions of $25\times25\times285$ mm for each mixture, following the ASTM C 157 standard [50]. Similar to the early age shrinkage assessment, only the SIFCON matrix was examined in this phase of the study. For the initial 24 h, the molds were covered with plastic sheets and kept at a temperature of 20 ($\pm1)\,^{\circ}\text{C}$. After demolding, the autogenous shrinkage specimens were placed inside a climate chamber set to a temperature of 20 $^{\circ}\text{C}$ and a relative humidity of 95 %. Additionally, the autogenous long-term shrinkage specimens were covered with aluminum foil to prevent any water loss. Conversely, the drying shrinkage specimens were placed inside another climate chamber adjusted to a temperature of 20 $^{\circ}\text{C}$ and relative humidity of 50 %.

The first measurements were taken on the 7th day, followed by regular interval measurements up to 90 days. The calculated shrinkage strains were added to the early-age shrinkage strains starting from the 7th day. A similar measurement approach has been successfully implemented in a previous study [51]. This approach allowed for the inclusion of shrinkage strains that could not be obtained using the conventional mortar bar method, especially within the first 24 h, leading to more realistic results. In both early and long-term measurement

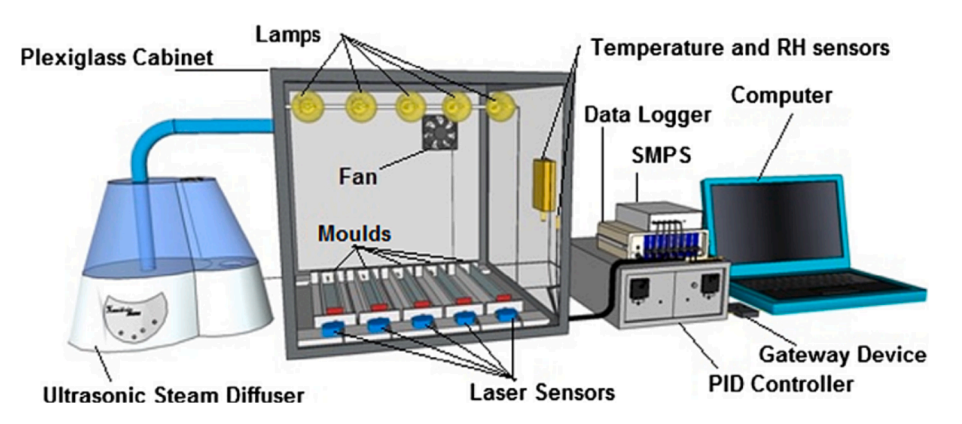


Fig. 2. Shrinkage measurement system (). adopted from [48]

methodologies, the entire surface areas of the specimens were sealed during the assessment of autogenous shrinkage strains. It can be posited that the conditions of the specimens were theoretically consistent across both measurement techniques for autogenous shrinkage. However, when considering drying shrinkage measurements, it is imperative to acknowledge that, owing to the intrinsic differences between the methods, the specimens had varying degrees of surface exposure. Specifically, early-age specimens were exposed on a single side, whereas long-term specimens were exposed on all sides. Consequently, the actual deformation of the SIFCON matrix might not align perfectly with the recorded long-term shrinkage strains in the context of drying shrinkage. However, it is postulated that the long-term shrinkage strains provide a lucid perspective for comparing the mixtures. Subsequent sections offer interpretations, taking these nuances into consideration, and comparisons are drawn based on relative changes.

2.5. Crack mapping

In this part of the study, SIFCON mixtures with fibers were used for crack mapping analysis. Plate-shaped specimens with dimensions of $25 \times 50 \times 305$ mm were employed, and three specimens were examined for crack mapping in each mixture. This specimen type has been used in previous SIFCON studies [52,53]. The selected specimen dimensions served two purposes. Firstly, they ensured that cracks would form in the narrow side and center of the specimen. Secondly, they maintained a constant surface area-to-volume ratio with the drying shrinkage specimens, as this ratio is known to have a significant effect on shrinkage strains due to differences in water evaporation [54].

All specimens were kept in a room with a temperature of 20 $^{\circ}$ C, and the molds were covered with plastic sheets to prevent plastic shrinkage cracks, as the aim of this study was to observe drying and autogenous shrinkage cracks. Subsequently, the specimens were demolded, and half of them were cured in lime-saturated water at 20 $^{\circ}$ C, while the other half were cured in a climate cabinet maintained at 20 $^{\circ}$ C and 50 $^{\circ}$ C relative humidity for 90 days.

At the age of 90 days, all specimens were removed from their curing environments and dried in the laboratory environment. At the time of experiments, the average RH of the lab environment is regularly checked and it is found to be 40.3 % (± 7.2). The purpose of this drying process was to simulate field drying after curing. By doing so, half of the

specimens were assumed to be sealed in the field for the long term, while the other half were left unsealed after one day. The lateral sides of the specimens were polished with 2500-grit sandpaper to facilitate better observation of the cracks. Before the examination, the polished sides of the specimens were wetted with ethanol. Due to the rapid evaporation of ethanol, cracks become more pronounced. This method was also beneficial for observing small cracks that may not be visible under dry conditions with a camera. The lateral center side of the specimens, limited to an area of $25 \times 25 \times 600$ mm (Fig. 3-a), was photographed using a high-resolution camera with the assistance of a powerful LED light (Fig. 3-b). Subsequently, the images were analyzed using ImageJ (Fiji version). The cracks were enhanced for better visibility by increasing the contrast, and the images were then converted to binary (Fig. 3-c). The percentage of cracked areas was calculated. It should be noted that since the crack widths were found to be very similar after prior examinations with a digital microscope, it was assumed that the percentages of cracked areas were not influenced by differences in crack width.

3. Results and discussions

3.1. Shrinkage

Fig. 4-a and Fig. 4-b present the early age and long-term shrinkage strains of the SIFCON matrixes under autogenous conditions, respectively. It can be observed that all mixtures exhibited very high shrinkage strains in the first few hours. After this initial period, a slight expansion was observed (Fig. 4-a). This phenomenon could be attributed to the crystallization pressure of calcium hydroxide or the re-absorption of bleeding water [55]. The persistent rise in shrinkage strains across all mixtures is somewhat surprising, as autogenous shrinkage typically culminates within the initial days. Nevertheless, given the high binder dosage and the low w/b ratio, reactions might still be ongoing. As expected, an increase in the SAP ratio resulted in a decrease in autogenous shrinkage strains. While the shrinkage strains of the mixtures with 60 kg/m³ additional water (SAP A 60 and SAP B 60) and the reference mixture remained almost constant after 1 day, the mixtures with 36 kg/ m³ additional water (SAP A 36 and SAP B 36) continued to shrink. It might be pointing out that 36 kg/m³ of additional water is not fully enough to compensate for water loss from hydration reactions. This phenomenon can be attributed to the inherent properties of high-

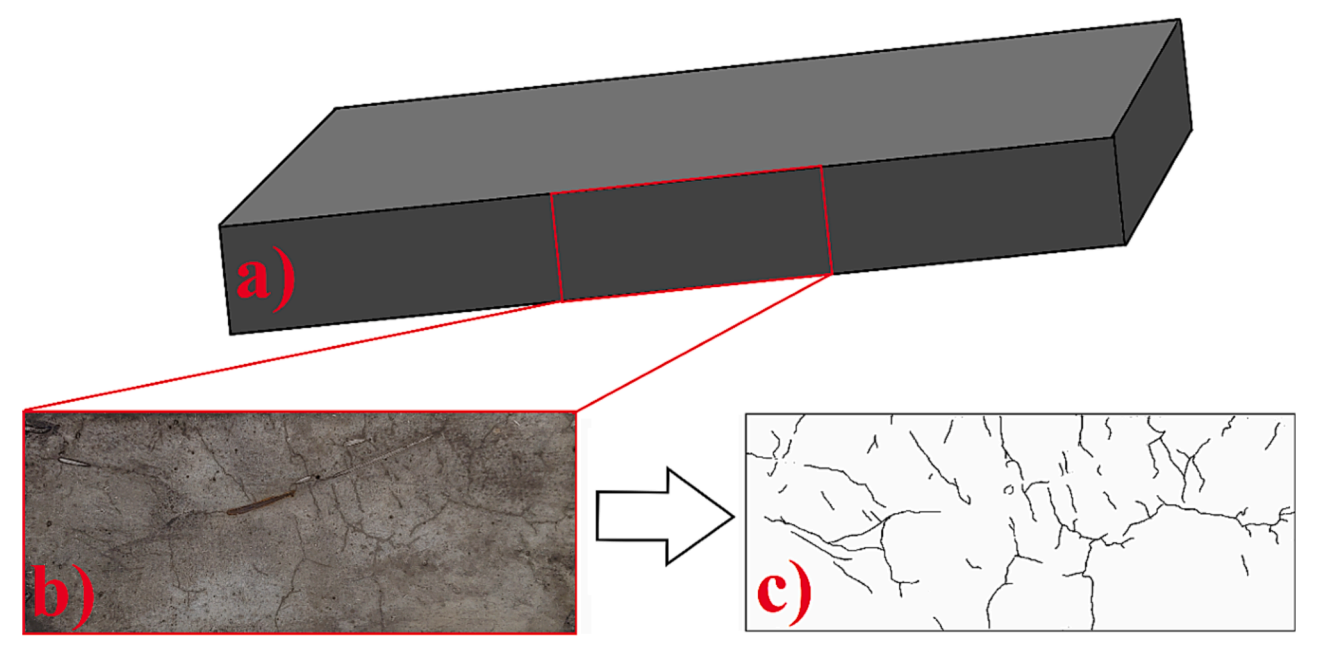


Fig. 3. Crack mapping procedure: a) examined area, b) polished and wetted surface, c) binary image of the surface.

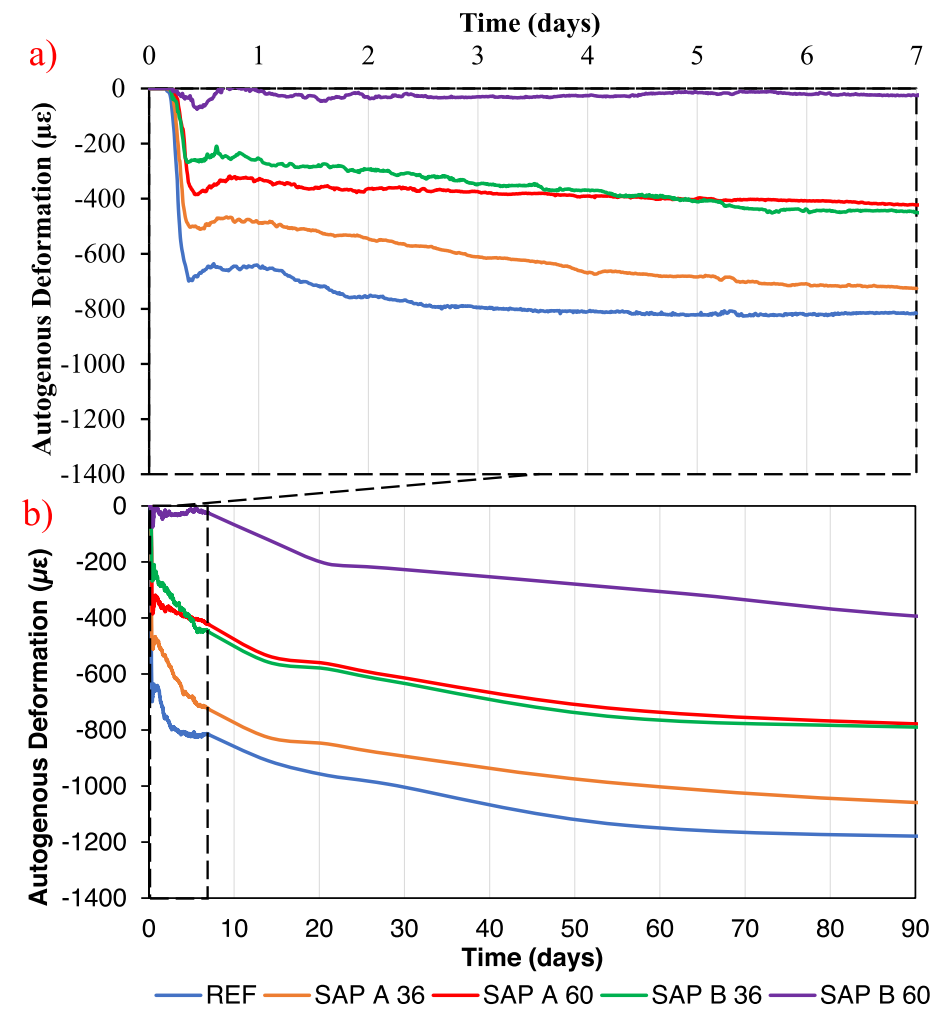


Fig. 4. Early age (a) and long-term (b) shrinkage deformations under autogenous conditions.

performance cement pastes, particularly the presence of silica fume which leads to significant chemical shrinkage [56]. Since Eq. (1) does not cover the supplementary cementitious materials, not including SF in calculations resulted in insufficient additional water.

Fig. 5-a and Fig. 5-b illustrate the early age and long-term shrinkage strains of the SIFCON matrixes under drying conditions, respectively. The reductions in shrinkage strains followed a similar pattern to the autogenous shrinkage strains, except for SAP A 60 and SAP B 36. In contrast to the autogenous shrinkage strains, SAP B 36 exhibited better performance than SAP A 60 under drying conditions. This observation suggests that the performance of SAPs is also influenced by ambient conditions. This is understandable since SAPs have unique absorption and desorption kinetics that are dependent on their size and the testing environment [23].

There is no specific limit value for shrinkage, and the critical point is reached when the shrinkage strains exceed the tensile strength [57]. Therefore, the critical shrinkage value varies for different concretes depending on their strength development and shrinkage characteristics. However, the effect of SAP can be evaluated with reductions in shrinkage relative to the REF mixture. The reduction percentages in shrinkage strains on the 7th day, relative to the REF mixture, under autogenous conditions were 11.1 % for SAP 36, 48.2 % for SAP A 60, 44.9 % for SAP B 36, and 95.3 % for SAP B 60 mixtures. Additionally, the reduction percentages under autogenous conditions on the 90th day were 9.6 % for SAP 36, 33.5 % for SAP A 60, 32.6 % for SAP B 36, and 65.9 % for SAP B 60 mixtures. As observed, SAP was notably more effective at the early stages in reducing shrinkage strains under

autogenous conditions. However, SAP exhibited poorer performance in terms of reducing shrinkage strains at the early stages under drying conditions. Specifically, shrinkage strain reduction on the 7th day was 12.3 % for SAP 36, 38.1 % for SAP A 60, 26.3 % for SAP B 36, and 46.7 % for SAP B 60 mixtures. Moreover, shrinkage strain reduction on the 90th day under drying conditions was 13.8 % for SAP 36, 44.1 % for SAP A 60, 30.7 % for SAP B 36, and 53.9 % for SAP B 60 mixtures.

The SAP A 36 mixture exhibited a lower reduction in shrinkage strains compared to the other mixtures, and there were no significant differences between early and long-term reductions. Additionally, when considering the same amount of internal curing water, SAP A was less effective than SAP B in reducing shrinkage strains under both autogenous and drying conditions. This suggests that the specific characteristics of SAPs, beyond just size, have a significant impact on internal curing performance. Zhong et al. (2019) [58] highlighted that the absorption behavior of SAPs can vary based on their chemical structures. Specifically, SAPs with high densities of anionic functional groups absorbed cement pore solution quickly but also released it rapidly due to interactions with multivalent cations in the pore solution, such as Ca²⁺. Furthermore, another study by Zhong et al. (2021) [59] emphasized the mechanisms of internal curing water release from different types of SAPs in cement paste, suggesting that the kinetics of water release and the distribution of SAPs in the mixture are crucial for their performance. Therefore, the differences observed between specimens containing SAP A and SAP B may stem from the kinetics of water release and particle distribution.

The better performance of SAP at the early stages under autogenous

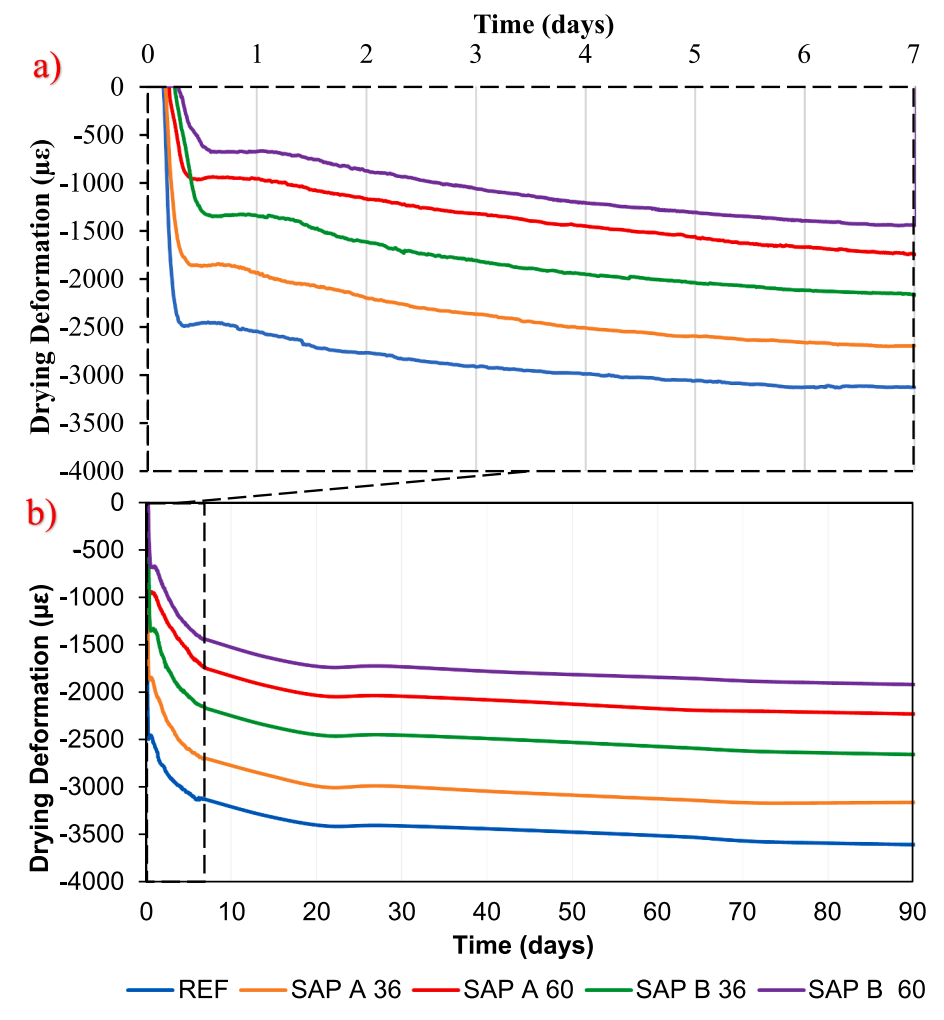


Fig. 5. Early age (a) and long-term (b) shrinkage deformations under drying conditions.

conditions is understandable, as the mechanism of internal curing aims to reduce shrinkage strains by supplying extra water to compensate for the water loss due to hydration reactions. On the other hand, SAP showed slightly better performance on the 90th day compared to the 7th day under drying conditions in terms of reducing shrinkage strains. This indicates that, although SAP reduced shrinkage strains for both ages, the availability of extra water slightly affected the shrinkage-reducing performance at the early stages due to increased evaporation. However, there could be more than one parameter influencing this behavior. This phenomenon will be discussed in detail in the following section.

3.2. Effectiveness of internal curing under drying conditions

There have been controversial reports in the literature regarding the effectiveness of internal curing under drying conditions. Some researchers have reported an increase in shrinkage under drying conditions [27,28], while others have reported contrary results [25,26]. This phenomenon has been explained by several reasons in the literature [31], including:

- 1. Easier water evaporation: Water absorbed by SAP has higher mobility, making it more prone to evaporation [60].
- Higher evaporation rate: Internal humidity in SAP-containing mixtures can be higher, leading to an increased RH difference between the specimen and the environment, resulting in higher evaporation rates [61].

3. More available water for evaporation: The additional internal curing water provides more water that can potentially evaporate [62].

The mechanisms behind this phenomenon are reasonable, but the controversial results in the literature may be attributed to the measurement technique and the ratio of shrinkage under drying conditions to shrinkage under autogenous conditions.

Plastic shrinkage typically begins within the first few hours and continues until the final setting [63]. Therefore, the time between the initial and final setting can be considered as the plastic shrinkage stage. In Fig. 6, shrinkage strains under drying conditions from the initial to final setting and from the final setting to the 7th day are presented. It can be observed that SAP is highly effective in reducing the shrinkage strains from the initial to final setting times. From the final setting to the 7th day, the REF mixture exhibited the least shrinkage strain. If the measurements were taken at 24 h as recommended in the ASTM C 157 standard [50], the shrinkage strains of SAP-containing mixtures would be higher than those of the REF mixture. This indicates that measurement techniques can lead to misleading results, especially when dealing with delicate phenomena like early-age shrinkage.

Internal curing is introduced to provide water for hydration reactions, thereby mitigating autogenous shrinkage [44]. It has also been found to be beneficial in terms of mitigating plastic shrinkage [9,10]. While achieving these benefits, side effects such as increased shrinkage under drying conditions may occur. To avoid such unwanted effects, the proportions of shrinkage strains under autogenous and drying conditions should be evaluated. In this study, the mean ratio of shrinkage

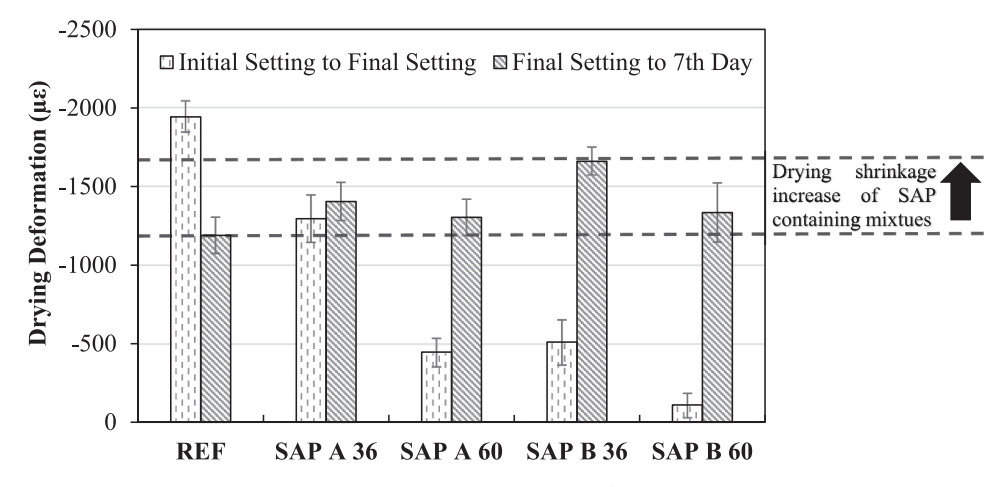


Fig. 6. Parts of shrinkage values at the early age.

under drying conditions to shrinkage under autogenous conditions was approximately 4.1. This ratio was sufficient to compensate for the side effects of SAP under drying conditions, as the shrinkage strains of the SAP-containing mixtures on the 7th day and the 90th day were lower than those of the REF mixture. However, depending on mixture characteristics such as water/binder ratio and binder dosage, the reduction in plastic shrinkage and autogenous shrinkage strains may not be enough to compensate for the increase in shrinkage strains under drying conditions.

Indeed, determining the specific contributions of plastic, drying, and autogenous shrinkage strains can be challenging, and it requires additional tests and analyses to differentiate between them accurately. However, based on the results presented in Fig. 6, it can be concluded that SAP has a significant effect in reducing the overall shrinkage under drying conditions, as it demonstrates high effectiveness from the initial setting until the final setting. As demonstrated in previous sections, SAP effectively reduced autogenous shrinkage. Consequently, it also positively impacts shrinkage strains under drying conditions. It is noteworthy that the size of the specimen significantly influences shrinkage. Therefore, further investigations and specific tests targeting individual shrinkage mechanisms and governing specimen sizes would be valuable to gain a more comprehensive understanding of how SAP influences different types of shrinkage and their magnitudes.

3.3. Crack mapping

A representative cracked surface shown in Fig. 7 clearly illustrates the presence of cracks predominantly around and between the fibers in the SIFCON matrix. It is important to note that SIFCON, which contains 10 % (by volume) randomly dispersed fibers, may have cracks that are not directly connected to the fibers visible on the surface. These cracks could potentially be connected to fibers located beneath the surface, emphasizing the complex crack pattern in SIFCON.

The observed crack pattern, described as "mapping-like cracks," is consistent with previous studies [64,65]. The cracking around and between fibers can be attributed to stress concentration in these regions caused by the shrinkage strains. As mentioned by Gilani [39], SIFCON tends to exhibit cracking between the fibers. This phenomenon is unique to SIFCON due to the combination of significant shrinkage strains induced by the nature of the SIFCON matrix and the presence of a rigid network formed by the fibers.

It is noteworthy that the specimens in this study were cured under non-restrained conditions, making the occurrence of cracking between fibers even more intriguing. Typically, the formation of cracks in concrete under non-restrained conditions is relatively uncommon. Yet, it could be said that specimens were restrained by fibers. The findings of cracking between fibers in this study provide valuable insights into the

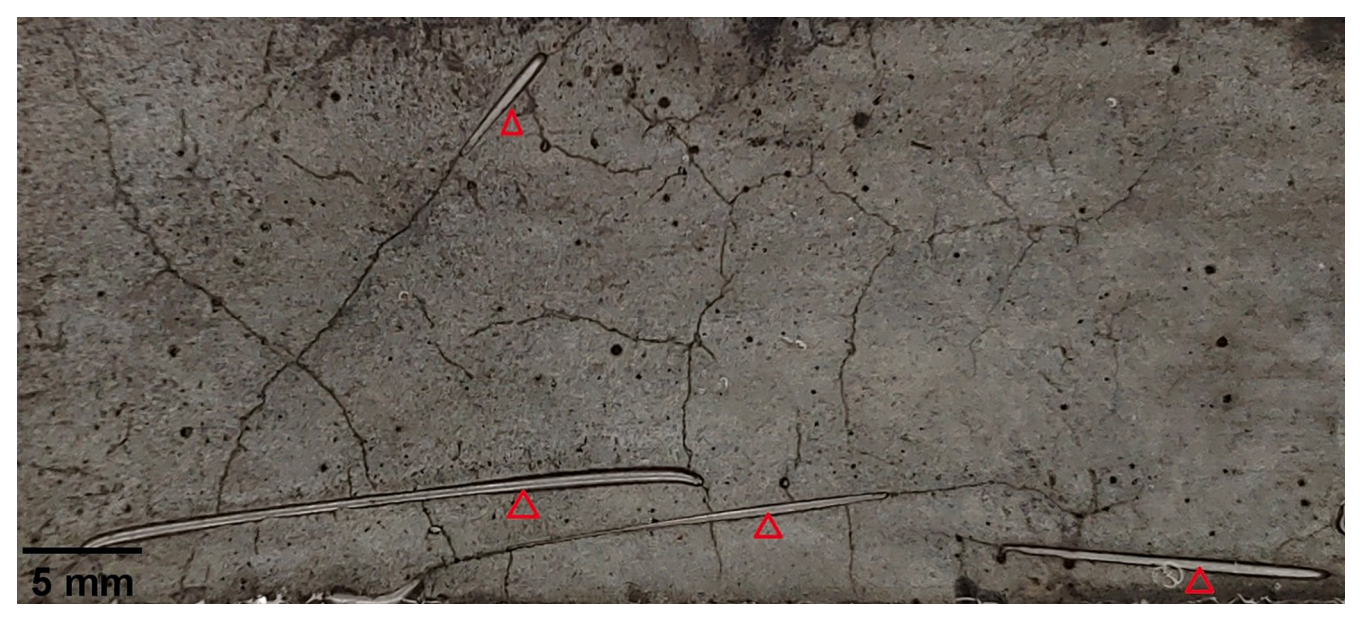


Fig. 7. Example of a cracked surface (Δ : fibers).

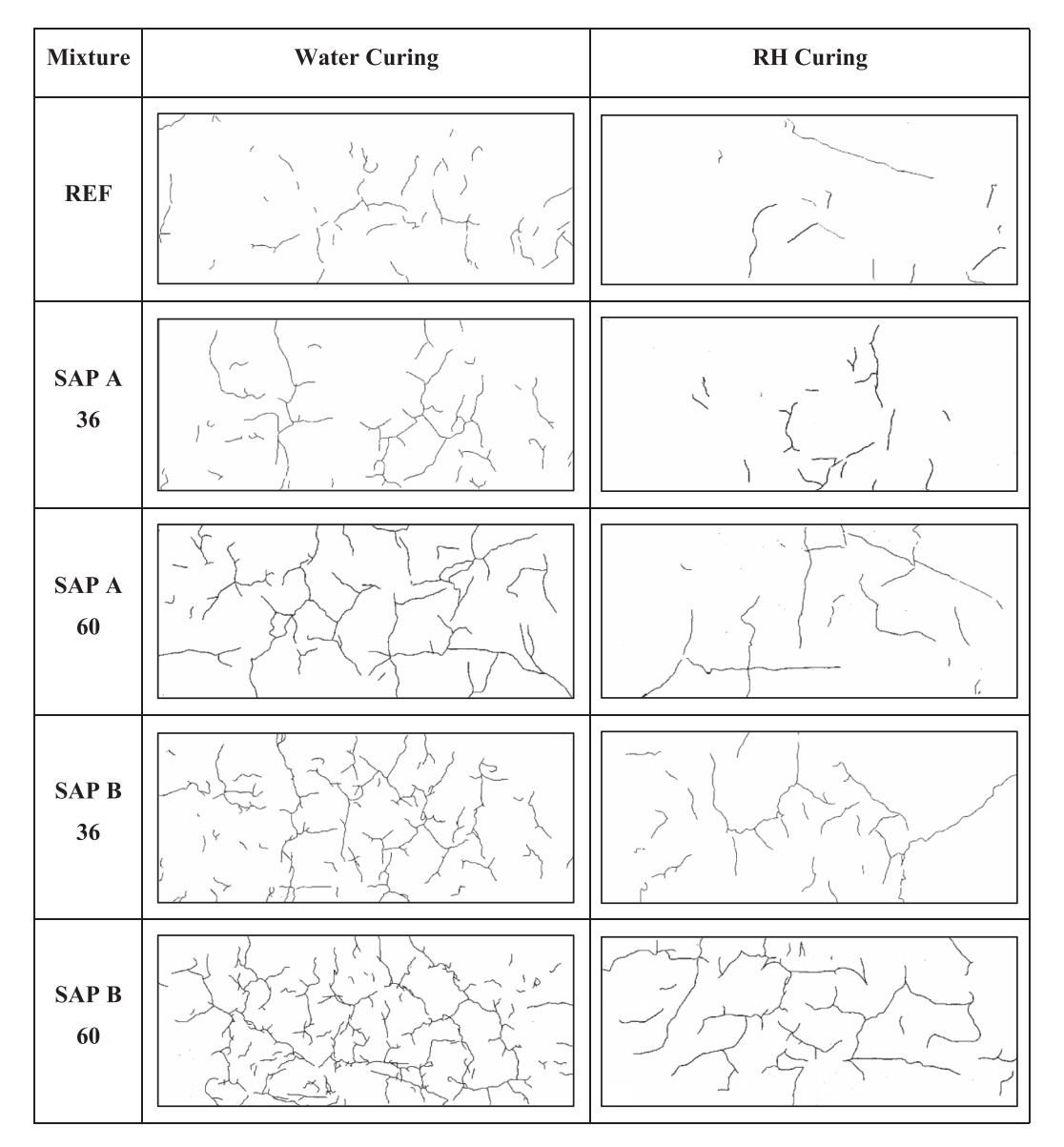


Fig. 8. Images of cracked surfaces.

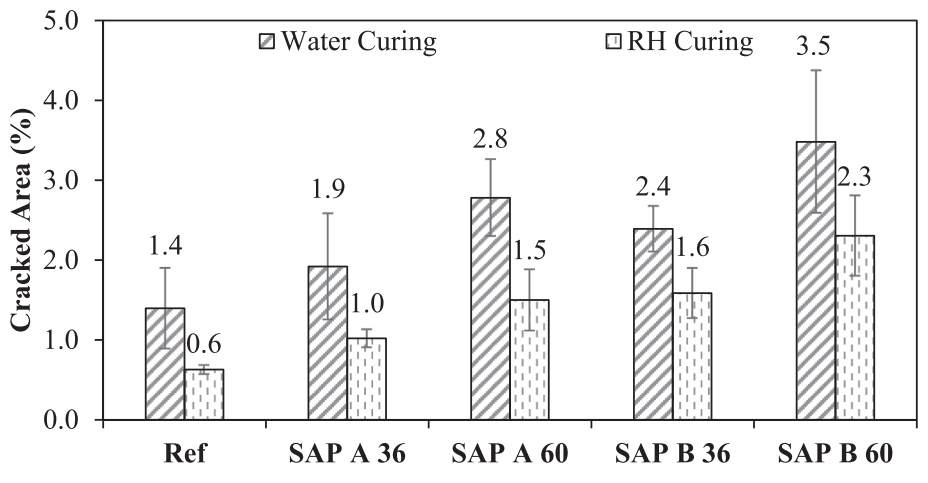


Fig. 9. Percentages of cracked areas.

behavior of SIFCON and highlight its unique characteristics in terms of crack formation and distribution.

The binary images of cracks in Fig. 8 and the corresponding mean percentages of cracked areas in Fig. 9 provide insights into the crack development in the different mixtures and under different curing conditions. The results show clear evidence of cracking induced by the use of SAP. As the SAP content increases, the cracks become more pronounced, and the cracked area expands.

It is important to note that these cracks, although present, might not appear to have a significant negative impact on the strength properties of the specimens. However, it is well-known that shrinkage cracking can lead to durability issues, primarily due to the increased diffusion of harmful substances through the cracks. Additionally, shrinkage cracks can facilitate the interconnection of capillary pores, further compromising the durability of the material [40].

Notably, significant differences were observed between water curing and RH curing. Contrary to expectations, the water-cured specimens exhibited more cracking compared to the RH-cured specimens. Several reasons may account for this difference, including increased cracking sensitivity due to strength loss, parasite strain development caused by the swelling of SAP, and the drying process of the water-cured specimens.

It is known that SAP can lead to strength loss due to an increased pore ratio, which might result in lower tensile strength, thus increasing cracking sensitivity. Additionally, long-term swelling of SAP in the water-cured specimens may contribute to this phenomenon. Considering the 90-day water curing period for the specimens, it is expected that the SAP remained swollen during the curing process. The utilization of SAP's absorption capacity was based on its behavior in cementitious environments, suggesting that during water curing, SAP is likely to absorb more, resulting in parasite strains within the matrix.

However, these effects are assumed to be minor. It seems that water movement during the drying process has a more dominant effect, as the non-SAP-containing reference specimens exhibited a similar pattern to the SAP-containing specimens. Consequently, water movement is found to be responsible for the cracking performance observed in the specimens mentioned above.

3.4. Effect of water movement on cracking

The findings show that cracking is strongly related to the usage of SAP, SAP content, SAP type, and curing environment. Due to the intricate nature of shrinkage and cracking, the aforementioned effects must be examined in three main parts: i) the increase in cracking in SAP-containing mixtures relative to REF mixtures, ii) the increase in cracking in SAP B-containing mixtures relative to SAP A-containing mixtures, iii) the increase in cracking in water-cured specimens related to RH-cured specimens.

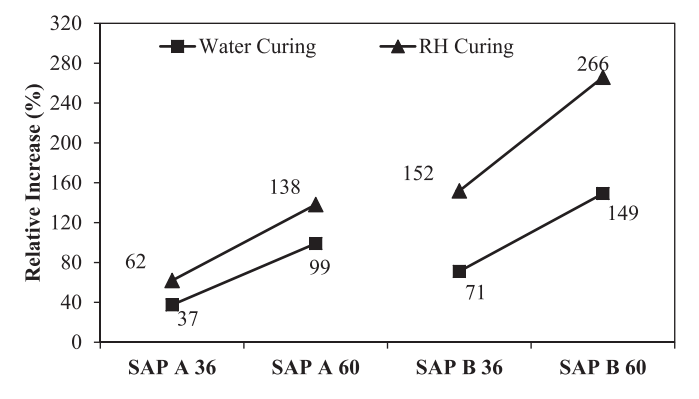


Fig. 10. Increase in cracked areas of SAP containing mixtures relative to REF mixtures.

3.4.1. Increase of cracking in SAP-containing mixtures

The increase in cracked areas of SAP-containing mixtures relative to their REF mixtures is presented in Fig. 10. When SAP A is used, cracking is increased by 37 % to 99 % in water-cured specimens and by 62 % to 138 % in RH-cured specimens. When SAP B is used, cracking is increased by 71 % to 149 % in water-cured specimens and by 152 % to 266 % in RH-cured specimens. The increase in cracking is observed with the increase in SAP and internal curing water content. The mechanisms of easier water evaporation [60], increased RH difference between the specimen and the environment [61], and more available water to evaporate [62], individually or in combination, are responsible for these increased cracked areas, as mentioned in Section 3.2. Once the water evaporates due to various reasons mentioned above, loose capillary pores become desiccated. This indicates that internal curing may lead to more cracking during the structure's life cycle if it is subjected to water movements such as wetting-drying and significant RH changes in the environment. It is known that wetting-drying can increase shrinkage due to viscoelastic relaxation [66]. Therefore, the inclusion of water reservoirs like SAP in concrete could result in more desiccation and shrinkage.

3.4.2. Increase of cracking in SAP B-containing mixtures

In both curing environments and with both additional internal curing water contents, specimens containing SAP B exhibited more cracking compared to specimens containing SAP A (Fig. 10). The main difference between SAP A and SAP B lies in their particle sizes and distributions. Although both SAP types have the same origin, the absorption and desorption kinetics can vary with particle size [67]. The evaporation rate is known to have a significant effect on plastic shrinkage [68], and it is also an important parameter for drying shrinkage. It is well-known that as the RH of the environment decreases, drying shrinkage strains increase [24]. The main mechanism behind this is the increased evaporation rate of the specimens due to the larger difference between the RH of the environment and the internal RH of the specimen. As mentioned in Section 3.2, the mechanism of increased RH difference between the specimen and the environment [61] appears to be more effective than other mechanisms in this context. Smaller particle-sized SAP tends to release water more quickly due to the larger surface area [67]. The prolonged drying time (or lower evaporation rate) of SAP B may have resulted in greater differences in shrinkage strains between the inner and outer sides of the specimens. Consequently, the prolonged drying time of SAP B-containing specimens likely contributed to increased cracking. Therefore, in addition to water content and water movement, the water absorption and desorption characteristics, as well as the particle size distribution of SAP, are also important factors to consider concerning cracking.

3.4.3. Increase of cracking in water-cured mixtures

The increase in cracked areas of water-cured specimens compared to RH-cured specimens is shown in Fig. 11. The REF mixture exhibited a

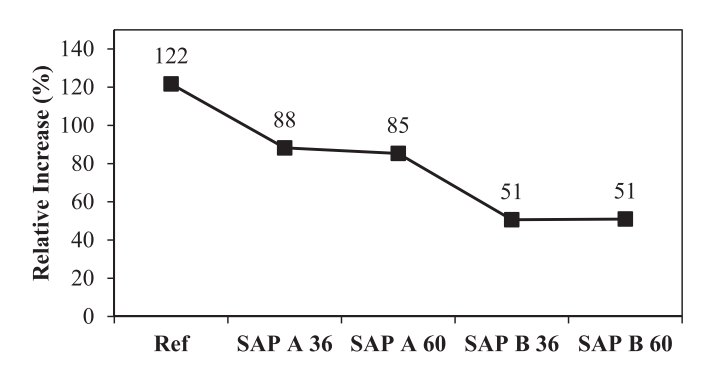


Fig. 11. Increase in cracked areas of water-cured specimens relative to RH-cured specimens.

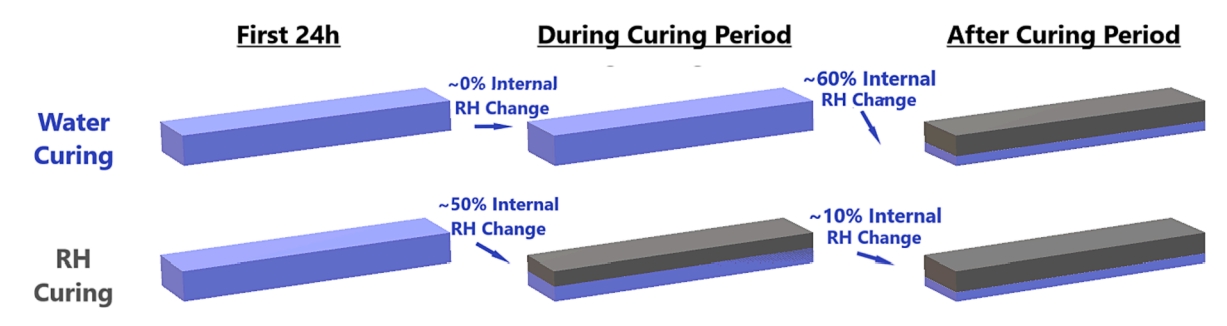


Fig. 12. Illustration of water and RH-cured specimens' internal RH change through the curing and crack mapping processes.

122 % increase in cracking after water curing. In contrast, SAP A-containing mixtures experienced an 85 % to 88 % increase in cracking, and SAP B-containing mixtures showed a 51 % increase. Although the cracked areas of SAP B-containing mixtures were higher than the other mixtures, they were less influenced by environmental conditions. This finding is consistent with the observed shrinkage strains of the mixtures (Fig. 4 and Fig. 5). However, as discussed earlier, SAP B is more affected by water movement. Therefore, the contrasting results suggest that shrinkage should be examined using different tests and test conditions to observe the side effects of shrinkage-reducing methods or agents.

The observation of more cracking in water-cured specimens compared to RH-cured specimens is unexpected. The illustration in Fig. 12 shows the internal RH change in both types of curing and during the crack mapping process. Water-cured specimens did not experience a drop in RH during the first 24 h and the curing period, but they lost 60 % of RH during the crack mapping process. In contrast, RH-cured specimens encountered RH drops both during curing and after the curing period, yet the drops were relatively smoother; approximately 50 % (from 100 % to 50 % RH) after the first 24 h and 10 % (from 50 % to 40 % RH) after the curing period. The rapid moisture loss in water-cured specimens may have led to increased cracking in these specimens. Particularly, rapid RH changes could induce stress relaxation. In concrete, stress relaxation means that when there is constant strain, internal stresses diminish over time. If these stresses don't relax properly, they can cause cracking [69]. Also, the connection between SAP content and cracking can be explained by stress relaxation. As more water evaporates from the specimen during drying, more voids are left, which can lead to increased stress relaxation. In addition to stress relaxation, the swelling of SAP during water curing might also negatively influence cracking. When SAP is saturated and swells in pore water, it reaches its maximum size for those conditions. However, during water curing, when SAP encounters lime-saturated water, it might try to absorb more water and expand, given that the pH of lime-saturated water is lower than that of the pore solution. This tendency of SAP to expand could introduce additional stresses. Regardless of the effect of SAP usage and content on cracking, as discussed earlier, all specimens exhibited an increase in cracked areas ranging from 51 % to 122 % (Fig. 11). This indicates that RH changes and change ratios also have a significant influence on cracking.

4. Conclusion

Based on the experimental study and analyses conducted, the following conclusions can be drawn:

- SAP is effective in reducing both autogenous and drying shrinkage strains, with a significant effect observed in the first few hours. This can be attributed to the substantial decrease in plastic shrinkage with the use of SAP during the early stages of hydration.
- The size of SAP particles plays an important role in mitigating shrinkage strains. Coarser SAP (SAP B) was found to be more effective in reducing shrinkage, but it also resulted in more cracking. This

- can be explained by the absorption and desorption characteristics of SAP, where coarser particles release water more quickly, leading to increased shrinkage strain differences within the specimen.
- Contradictory reports on the performance of internal curing agents in drying shrinkage strains may be attributed to the measurement techniques and the proportion of different types of shrinkage. Measurements starting from the final setting or one day after may be misleading due to the significant reduction in shrinkage strains caused by SAP during the first few hours. Evaluating the all side-effects of SAP is important to accurately assess the benefits of SAP.
- The negative effects of SAP on drying shrinkage can be compensated
 by reductions in autogenous and plastic shrinkage at early ages. The
 ratio of shrinkage strains under drying conditions to shrinkage
 strains under autogenous conditions is crucial for assessing the
 compensation of negative effects. Therefore, the proportion of
 different types of shrinkage should be considered to avoid an increase in drying shrinkage.
- Crack mapping revealed that, cracks can form due to shrinkage strains between fibers in SIFCON. This indicates the importance of considering the presence and behavior of fibers in assessing cracking potential.
- RH-cured specimens displayed fewer cracks compared to those cured in water. The rapid change in RH can be posited as the potential cause. Given the accelerated RH change in water-cured specimens, stress relaxation occurred, and insufficient time was available for adjustment, possibly leading to increased cracking.

These conclusions highlight the complex nature of shrinkage and cracking phenomena and emphasize the need for careful consideration of various factors, such as SAP characteristics, curing conditions, and measurement techniques, to accurately assess and mitigate cracking potential in UHPC.

5. Declaration of generative AI and AI-assisted technologies in the writing process

During the preparation of this work the author(s) used ChatGPT in order to proof-read the manuscript. After using this tool/service, the author(s) reviewed and edited the content as needed and take(s) full responsibility for the content of the publication.

CRediT authorship contribution statement

Bayram Tutkun: Writing – original draft, Visualization, Validation, Resources, Methodology, Investigation, Data curation, Conceptualization. Ege Su Barlay: Writing – review & editing, Validation, Investigation, Methodology. Çağlar Yalçınkaya: Writing – review & editing, Supervision, Methodology, Conceptualization. Halit Yazici: Writing – review & editing, Supervision, Project administration, Methodology, Funding acquisition, Conceptualization.

Declaration of Competing Interest

The authors declare the following financial interests/personal relationships which may be considered as potential competing interests: Bayram Tutkun reports financial support was provided by Scientific and Technological Research Council of Turkey.

Data availability

Data will be made available on request.

Acknowledgments

The authors would like to acknowledge the financial support provided by The Scientific & Technological Research Council of Türkiye (TÜBİTAK, Project No: 121M181). They are also grateful to Pomza Export (Türkiye), Dere Beton (Türkiye), SNF Floerger (France) for the material support. The authors are also grateful to Dr. Ahsanollah BEGLARIGALE, Ms. Çiğdem YETİŞ and Mr. Engin ATEŞMEN for their assistance in theoretical and experimental studies.

References

- K.L. Scrivener, R.J. Kirkpatrick, Innovation in use and research on cementitious material, Cem. Concr. Res. 38 (2008) 128–136, https://doi.org/10.1016/j. cemconres 2007 09 025
- [2] D. Pavan Kumar, S. Amit, M. Sri Rama Chand, Influence of various nano-size materials on fresh and hardened state of fast setting high early strength concrete [FSHESC]: A state-of-the-art review, Constr. Build. Mater. 277 (2021) 122299, https://doi.org/10.1016/j.conbuildmat.2021.122299.
- [3] H. Zhang, Z. Wu, X. Hu, X. Ouyang, Z. Zhang, N. Banthia, C. Shi, Design, production, and properties of high-strength high-ductility cementitious composite (HSHDCC): A review, Compos. B Eng. 247 (2022) 110258, https://doi.org/10.1016/j.compositesb.2022.110258.
- [4] R. Ranade, V.C. Li, W.F. Heard, B.A. Williams, Impact resistance of high strength-high ductility concrete, Cem. Concr. Res. 98 (2017) 24–35, https://doi.org/10.1016/j.cemconres.2017.03.013.
- [5] S. Ghourchian, Plastic Shrinkage Cracking in Concrete: From Mechanisms to Mitigation Strategies [Doctoral dissertation, ETH Zurich], 2018.
- [6] H. Huang, G. Ye, Examining the "time-zero" of autogenous shrinkage in high/ultrahigh performance cement pastes, Cem. Concr. Res. 97 (2017) 107–114, https://doi. org/10.1016/j.cemconres.2017.03.010.
- [7] C. Di Bella, Drying shrinkage of cementitious materials at early age [Doctoral dissertation, ETH Zurich], 2016.
- [8] S. Ghourchian, M. Wyrzykowski, L. Baquerizo, P. Lura, Performance of passive methods in plastic shrinkage cracking mitigation, Cem. Concr. Compos. 91 (2018) 148–155, https://doi.org/10.1016/j.cemconcomp.2018.05.008.
- [9] W. Boshoff, V. Mechtcherine, D. Snoeck, C. Schröfl, N. De Belie, A.B. Ribeiro, D. Cusson, M. Wyrzykowski, N. Toropovs, P. Lura, The effect of superabsorbent polymers on the mitigation of plastic shrinkage cracking of conventional concrete, results of an inter-laboratory test by RILEM TC 260-RSC, Mater. Struct./Mater. Constr. 53 (2020), https://doi.org/10.1617/s11527-020-01516-6.
- [10] D. Snoeck, B. Moerkerke, A. Mignon, N. De Belie, In-situ crosslinking of superabsorbent polymers as external curing layer compared to internal curing to mitigate plastic shrinkage, Constr. Build. Mater. 262 (2020), 120819, https://doi. org/10.1016/j.conbuildmat.2020.120819.
- [11] R. Henkensiefken, P. Briatka, D. Bentz, T. Nantung, J. Weiss, Plastic Shrinkage Cracking in Internally Cured Mixtures Made with Pre-wetted Lightweight Aggregate, Concr. Int. 32 (2) (2010) 49–54.
- [12] S.T. Lin, R. Huang, Effect of viscosity modifying agent on plastic shrinkage cracking of cementitious composites, Mater. Struct./Mater. Constr. 43 (2010) 651–664, https://doi.org/10.1617/s11527-009-9518-7.
- [13] P. Lura, B. Pease, G.B. Mazzotta, F. Rajabipour, J. Weiss, Influence of shrinkage-reducing admixtures on development of plastic shrinkage cracks, ACI Mater. J. 104 (2007) 187–194. https://doi.org/10.14359/18582.
- [14] D. Bentz, J. Weiss, Internal Curing: A 2010 State-of-the-Art Review, NIST Interagency/Internal Report (NISTIR), National Institute of Standards and Technology, Gaithersburg, MD (2011), [online], https://doi.org/10.6028/NIST. IB 7765
- [15] L. Yang, C. Shi, Z. Wu, Mitigation techniques for autogenous shrinkage of ultrahigh-performance concrete – A review, Compos. B Eng. 178 (2019), 107456, https://doi.org/10.1016/j.compositesb.2019.107456.
- [16] N.P. Tran, C. Gunasekara, D.W. Law, S. Houshyar, S. Setunge, A. Cwirzen, A critical review on drying shrinkage mitigation strategies in cement-based materials, J. Build. Eng. 38 (2021), 102210, https://doi.org/10.1016/j.jobe.2021.102210.
- [17] S. Tang, D. Huang, Z. He, A review of autogenous shrinkage models of concrete, J. Build. Eng. 44 (2021), 103412, https://doi.org/10.1016/j.jobe.2021.103412.

- [18] D.P. Bentz, O.M. Jensen, Mitigation strategies for autogenous shrinkage cracking, Cem. Concr. Compos. 26 (2004) 677–685, https://doi.org/10.1016/S0958-9465 (03)00045-3
- [19] R.E. Philleo, Concrete Science and Reality, American Ceramic Society, Westerville, OH, 1991. http://ci.nii.ac.jp/naid/10014912076/en/ (accessed January 29, 2022).
- [20] O.M. Jensen, P. Lura, Techniques and materials for internal water curing of concrete, Mater. Struct./Mater. Constr. 39 (2006) 817–825, https://doi.org/ 10.1617/s11527-006-9136-6.
- [21] M. Tsuji, A. Okuyama, K. Enoki, S. Suksawang, Development of new concrete admixture preventing from leakage of water through cracks, JCA Proc. Cem. Concr. (Japan Cem. Assoc.) 52 (1998) 418–423.
- [22] O.M. Jensen, P.F. Hansen, Water-entrained cement-based materials II. Experimental Observations, Cem. Concr. Res. 32 (2002) 647–654, https://doi.org/ 10.1016/s0008-8846(01)00463-x.
- [23] C. Schröfl, V. Mechtcherine, M. Gorges, Relation between the molecular structure and the efficiency of superabsorbent polymers (SAP) as concrete admixture to mitigate autogenous shrinkage, Cem. Concr. Res. 42 (2012) 865–873, https://doi. org/10.1016/j.cemconres.2012.03.011.
- [24] A. Hajibabaee, M.T. Ley, The impact of wet curing on curling in concrete caused by drying shrinkage, Mater. Struct./Mater. Constr. 49 (2016) 1629–1639, https://doi. org/10.1617/s11527-015-0600-z.
- [25] J. Yang, L. Liu, Q. Liao, J. Wu, J. Li, L. Zhang, Effect of superabsorbent polymers on the drying and autogenous shrinkage properties of self-leveling mortar, Constr. Build. Mater. 201 (2019) 401–407, https://doi.org/10.1016/j. conbuildmat.2018.12.197.
- [26] S. Mönnig, H.W. Reinhardt, Results of a comparative study of the shrinkage behaviour of concrete and mortar mixtures with different internal water sources, in: International RILEM Conference on Volume Changes of Hardening Concrete: Testing and Mitigation, RILEM Publications SARL, 2006, pp. 67–75.
- [27] V. Mechtcherine, L. Dudziak, S. Hempel, Mitigating early age shrinkage of ultrahigh performance concrete by using super absorbent polymers (SAP). Proceedings of the Creep, Shrinkage, and Durability, Mechanics of Concrete and Concrete Structures (2009) 847–853.
- [28] A.M. Soliman, M.L. Nehdi, Effect of partially hydrated cementitious materials and superabsorbent polymer on early-age shrinkage of UHPC, Constr. Build. Mater. 41 (2013) 270–275, https://doi.org/10.1016/j.conbuildmat.2012.12.008.
- [29] J. Zhang, Y.D. Han, Y. Gao, Y. Luosun, Integrative Study on the Effect of Internal Curing on Autogenous and Drying Shrinkage of High-Strength Concrete, Drying Technol. 31 (2013) 565–575, https://doi.org/10.1080/07373937.2012.745869.
- [30] J. Yang, Y. Guo, A. Shen, Z. Chen, X. Qin, M. Zhao, Research on drying shrinkage deformation and cracking risk of pavement concrete internally cured by SAPs, Constr. Build. Mater. 227 (2019), 116705, https://doi.org/10.1016/j. conbuildmat.2019.116705.
- [31] J. Liu, C. Shi, X. Ma, K.H. Khayat, J. Zhang, D. Wang, An overview on the effect of internal curing on shrinkage of high performance cement-based materials, Constr. Build. Mater. 146 (2017) 702–712, https://doi.org/10.1016/j. conbuildmat 2017 04 154
- [32] M. Wyrzykowski, P. Lura, F. Pesavento, D. Gawin, Modeling of Water Migration during Internal Curing with Superabsorbent Polymers, J. Mater. Civ. Eng. 24 (2012) 1006–1016, https://doi.org/10.1061/(asce)mt.1943-5533.0000448.
- [33] Ç. Yalçınkaya, A. Beglarigale, H. Yazıcı, The effect of metakaolin and end type of steel fiber on fiber-SIFCON matrix bond characteristics, Usak Univ. J. Mater. Sci. 3 (2014) 97. https://doi.org/10.12748/uujms.201416504.
- [34] J.R. Homrich, A.E. Naaman, Stress-Strain Properties of SIFCON in Compression, Spec. Publ. 105 (1987) 283–304. https://doi.org/10.14359/2172.
- [35] M. Tuyan, H. Yazıcı, H. Yazıcı, Pull-out behavior of single steel fiber from SIFCON matrix, Constr. Build. Mater. 35 (2012) 571–577, https://doi.org/10.1016/j.conbuildmat.2012.04.110.
- [36] K. Armagan, M. Canbaz, Effect of Fiber Type on Freeze Thaw Durability of SIFCON, Int. J. Adv. Mech. Civil Eng. 3 (2016) 56–59.
- [37] P. Deepesh, J. Kanase, Study the Influence of Magnesium Sulphate Attack on SIFCON by Partial Replacement of Cement with Fly Ash, Int. J. Innovat. Res. Sci. Technol. 3 (2016) 312-315.
- [38] M.F. Alrubaie, S.A. Salih, W.A. Abbas, Durability of Slurry Infiltrated Fiber Concrete to Corrosion in Chloride Environment: An Experimental Study, Part I, International Journal of Civil and Environmental Engineering 13 (2019) 502–508, https://doi.org/10.5281/zenodo.3455681.
- [39] A.M. Gilani, Various durability aspects of slurry infiltrated fiber concrete, Middle East Technical University (2007).
- [40] N. Hearn, Effect of shrinkage and load-induced cracking on water permeability of concrete, ACI Mater. J. 96 (1999) 234–241. https://doi.org/10.14359/450.
- [41] B. Tutkun, H. Yazıcı, Effect of absorption determining methods of superabsorbent polymers in cementitious environments on the fresh properties, Mater. Today:. Proc. (2022) 43–49, https://doi.org/10.1016/j.matpr.2022.11.403.
- [42] G. Lefever, E. Tsangouri, D. Snoeck, D.G. Aggelis, N. De Belie, S. Van Vlierberghe, D. Van Hemelrijck, Combined use of superabsorbent polymers and nanosilica for reduction of restrained shrinkage and strength compensation in cementitious mortars, Constr. Build. Mater. 251 (2020), 118966, https://doi.org/10.1016/j.co nbuildmat.2020.118966.
- [43] J. Han, H. Fang, K. Wang, Design and control shrinkage behavior of high-strength self-consolidating concrete using shrinkage-reducing admixture and superabsorbent polymer, J Sustain Cem Based Mater. 3 (2014) 182–190, https://doi. org/10.1080/21650373.2014.897268.

- [44] O.M. Jensen, P.F. Hansen, Water-entrained cement-based materials I. Principles and Theoretical Background, Cem. Concr. Res. 31 (2001) 647–654, https://doi. org/10.1016/S0008-8846(01)00463-X.
- [45] TS EN 1015-3. Methods of test for mortar for masonry-Part 3: Determination of consistence of fresh mortar (by flow table). Ankara, Turkey: Turkish Standard Institute; 2000 [in Turkish].
- [46] European federation of producers and contractors of specialist products for structures (EFNARC). Specifications and guidelines for self-compacting concrete; 2005
- [47] L.P. Esteves, P. Cachim, V.M. Ferreira, in: Advances in Construction Materials, 2007, pp. 451–462, https://doi.org/10.1007/978-3-540-72448-3_45.
- [48] Ç. Yalçınkaya, H. Yazıcı, Effects of ambient temperature and relative humidity on early-age shrinkage of UHPC with high-volume mineral admixtures, Constr. Build. Mater. 144 (2017) 252–259, https://doi.org/10.1016/j.conbuildmat.2017.03.198.
- [49] Ç. Yalçınkaya, H. Yazıcı, Early-age shrinkage properties of eco-friendly reactive powder concrete with reduced cement content, Eur. J. Environ. Civ. 26 (2019) 456–472, https://doi.org/10.1080/19648189.2019.1665105.
- [50] ASTM. "ASTM C157/C157M 17: Standard Test Method for Length Change of Hardened Hydraulic-Cement Mortar and Concrete." 2017.
- [51] C. Yalçınkaya, B. Felekoğlu, H. Yazıcı, Influence of aggregate volume on the shrinkage, rheological and mechanical properties of ultra-high performance concrete, J. Fac. Eng. Archit. Gazi Univ. 35 (2020) 1701–1718. https://doi. org/10.17341/gazimmfd.449285.
- [52] A. Beglarigale, Ç. Yalçınkaya, H. Yiğiter, H. Yazıcı, Flexural performance of SIFCON composites subjected to high temperature, Constr. Build. Mater. 104 (2016) 99–108, https://doi.org/10.1016/j.conbuildmat.2015.12.034.
- [53] H. Yazici, H. Yiğiter, S. Aydin, B. Baradan, Autoclaved SIFCON with high volume Class C fly ash binder phase, Cem. Concr. Res. 36 (2006) 481–486, https://doi.org/ 10.1016/j.cemconres.2005.10.002.
- [54] N. Jafarifar, K. Pilakoutas, T. Bennett, Moisture transport and drying shrinkage properties of steel-fibre-reinforced-concrete, Constr. Build. Mater. 73 (2014) 41–50, https://doi.org/10.1016/j.conbuildmat.2014.09.039.
- [55] G. Sant, B. Lothenbach, P. Juilland, G. Le Saout, J. Weiss, K. Scrivener, The origin of early age expansions induced in cementitious materials containing shrinkage reducing admixtures, Cem. Concr. Res. 41 (2011) 218–229, https://doi.org/ 10.1016/j.cemconres.2010.12.004.
- [56] P. Lura, O. Mejlhede Jensen, K. Van Breugel, Autogenous shrinkage in highperformance cement paste: An evaluation of basic mechanisms, Cem Concr Res. 33 (2003) 223–232.

- [57] V. Gribniak, G. Kaklauskas, R. Kliukas, R. Jakubovskis, Shrinkage effect on short-term deformation behavior of reinforced concrete When it should not be neglected, Mater. Des. 51 (2013) 1060–1070, https://doi.org/10.1016/j.matdes 2013.05.028
- [58] P. Zhong, M. Wyrzykowski, N. Toropovs, L. Li, J. Liu, P. Lura, Internal curing with superabsorbent polymers of different chemical structures, Cem. Concr. Res. 123 (2019), 105789, https://doi.org/10.1016/j.cemconres.2019.105789.
- [59] P. Zhong, Z. Hu, M. Griffa, M. Wyrzykowski, J. Liu, P. Lura, Mechanisms of internal curing water release from retentive and non-retentive superabsorbent polymers in cement paste, Cem. Concr. Res. 147 (2021), 106494, https://doi.org/10.1016/j.ce mconres.2021.106494.
- [60] A. Assmann, Physical properties of concrete modified with superabsorbent polymers, [Doctoral Dissertation, Stuttgart University], 2013.
- [61] X. Ma, Y. Zhang, S. Wu, Effect of super absorbent polymer on the properties of cement mortar with high water-cement ratio, Concrete 7 (2015) 124–127.
- [62] A. Gonzalez-Corominas, M. Etxeberria, Effects of using recycled concrete aggregates on the shrinkage of high performance concrete, Constr. Build. Mater. 115 (2016) 32–41, https://doi.org/10.1016/j.conbuildmat.2016.04.031.
- [63] K. Kovler, S. Zhutovsky, Overview and future trends of shrinkage research, Materials and Structures/Materiaux et Constructions 39 (2006) 827–847, https://doi.org/10.1617/s11527-006-9114-z.
- [64] T. Shiotani, J. Bisschop, J.G.M. Van Mier, Temporal and spatial development of drying shrinkage cracking in cement-based materials, Eng. Fract. Mech. 70 (2003) 1509–1525, https://doi.org/10.1016/S0013-7944(02)00150-9.
- [65] J. Bisschop, J.G. van Mier, Effect of aggregates on drying shrinkage microcracking in cement-based composites, Materials and Structures/Materiaux et Constructions 35 (2002) 453–461, https://doi.org/10.1007/BF02483132.
- [66] G.W. Scherer, Drying, Shrinkage, and Cracking of Cementitious Materials, Transp. Porous Media 110 (2015) 311–331, https://doi.org/10.1007/s11242-015-0518-5.
- [67] Q. Jiang, K. Wan, Improving internal curing efficiency through adjusting ab- and desorption curve of superabsorbent polymer in cement pastes using sodium carbonate, Cem. Concr. Compos. 129 (2022), 104467, https://doi.org/10.1016/j. cemconcomp.2022.104467.
- [68] P.J. Uno, Plastic shrinkage cracking and evaporation formulas, ACI Mater. J. 95 (1998) 365–375. https://doi.org/10.14359/379.
- [69] A.B. Hossain, J. Weiss, Assessing residual stress development and stress relaxation in restrained concrete ring specimens, Cem. Concr. Compos. 26 (2004) 531–540, https://doi.org/10.1016/S0958-9465(03)00069-6.